Dalton Transactions

Accepted Manuscript

ROYAL SOCIETY OF CHEMISTRY

www.rsc.org/dalton

Cite this: DOI: 10.1039/c0xx00000x

www.rsc.org/xxxxxx

ARTICLE TYPE

Influence of Vanadium Concentration and Temperature on the Preparation of Electrochromic Thin Films of Ammonium Intercalated Vanadium(V) Oxide Xerogel Nanoribbons

Metodija Najdoski,[a*] Violeta Koleva [b] and Aksu Samet [a]

Received (in XXX, XXX) Xth XXXXXXXXX 20XX, Accepted Xth XXXXXXXXX 20XX
DOI: 10.1039/b000000x

A new and simple chemical method for deposition of thin films of ammonium intercalated $V_2O_5 \cdot nH_2O$ xerogels has been designed. The chemical deposition has been performed in aqueous solutions of ammonium metavanadate and acetic acid at temperatures between 50 and 85 °C. Depending on the vanadium concentration and deposition temperature xerogels with different composition have been prepared. The structure, morphology, electrochemical and electrochromic behaviour of the thin films with a composition of $(NH_4)_{0.15}V_2O_5 \cdot 1.3H_2O$ have been examined. The film morphology comprises randomly oriented ribbon-like units (100 nm wide and about 500 nm long) which are composed of aggregated primary smaller particles in the nanoscale region of 50–100 nm. Two relatively stable redox pairs are observed in the cyclic voltammograms which correspond to the two-step electrochromism with colour transformations yellow/green and green/blue. The thin film thickness is found to have strong influence on the transmittance variance as deduced by the optical spectra of the reduced and oxidized states. The best result regarding the transmittance variance of 54% at 400 nm is achieved with thin films with thickness of about 200 nm which makes the prepared films very attractive for application in electrochromic devices.

Introduction

Due to numerous applications the electrochromic materials are currently attracting a great deal of academic and commercial interest. Among the inorganic electrochromics tungsten(VI) oxide is known to show excellent electrochromic characteristics,[1] but its colour range is limited in the reversible transition of colourless to blue state. To extend the range of functions of electrochromics the latest trends in the commercial applications of the electrochromic materials are demanding increase in the colour palette demonstrated by the materials.[2] This is partly achieved by the use of organic electrochromics.[3] However, the organic electrochromics have a disadvantage compared to the inorganic ones related to the deterioration effect of the UV radiation. Vanadium(V) oxides display several colours related to the different vanadium oxidation states: yellow (V(V)), blue (V(IV)), green (V(III) or mixture of V(V) and V(IV)) and violet (V(II)).[4] Thus, among the inorganic electrochromic materials vanadium(V) oxides being polyelectrochromic have the potential to increase the colour palette, which makes them very attractive materials for different electrochromic devices.

Vanadium(V) oxide xerogels, expressed by $V_2O_5 \cdot nH_2O$, are known to be very reactive materials with rich intercalation chemistry, electronic and ionic conductivity, and electrochromic properties.[2] Due to the large lithium intercalation capacity the thin films of $V_2O_5 \cdot nH_2O$ gels have been used as antistatic coatings in the photographic industry,[5] humidity sensors,[5] microbatteries,[5] reversible cathodes for lithium ion batteries,[6,7] supercapacitors,[8] cathodes in electrochromic devices,[5,9-11] electrochromic mirrors.[10,11] Most recently, Costa et al. reported that the electrochromic cell based on an inkjet printed vanadium oxide xerogel on flexible PET/ITO electrode exhibits excellent colour contrast between different redox states and excellent cycling stability (more than 30 000 cycles with a degradation of 18%) which characteristics make it very promising for application in intelligent windows.[2]

Vanadium(V) oxide xerogels (solids and thin films) are most often prepared by sol-gel method in three main variants (using three synthetic routes): acidification of metavanadate aqueous solutions,[5,10,12] hydrolysis condensation of alkoxides[5,7,13,14] and reaction between H_2O_2 and V_2O_5 powder.[2,15] Other methods such as hydrothermal,[16] sputtering,[17,18] electrodeposition,[19] laser ablation technique,[20] inkjet printing,[2] etc. are also reported.

To the best of our knowledge there is no published chemical bath deposition method (CBD) for vanadium(V) oxide xerogels. It is well known that the chemical bath deposition method is a simple and low cost method that allows deposition of thin films on odd shape objects. Due to the low synthesis temperature, it can be used for deposition onto polymer substrates. Recently we have developed CBD methods for the preparation of thin films of sodium vanadium bronzes[21] and manganese oxides[22,23] and good results regarding the transmittance variance of the thin films have been obtained.

In this paper we report a new CBD method for production of $V_2O_5 \cdot nH_2O$ xerogel thin films with electrochromic properties using the synthetic approach of acidification of metavanadate

aqueous solutions. In our method we have used ammonium metavanadate and acetic acid. Besides the simplicity, our method enables preparation of ammonium intercalated vanadium oxide xerogels with different composition, and hence with different electrochromic properties, by variation of two experimental parameters: the metavanadate concentration and temperature. The structure, morphology, electrochemical and electrochromic behaviour are studied by various techniques such as X-ray powder diffraction, IR spectroscopy, TG-DTA analyses, SEM, AFM, cyclic voltammetry and UV-Vis spectrometry.

Experimental

Synthesis of Ammonium Intercalated Vanadium(V) Oxide Xerogels

Vanadium(V) oxide xerogels are synthesized *via* the acidification of aqueous solutions of NH_4VO_3 with varying concentration by acetic acid at different temperatures. The precipitation is performed in two ways: in presence or not of ethanol. The use of ethanol was provoked by the idea that ethanol, being salting out and dehydrating reagent, could influence the formation of precipitates with different composition (mainly in respect to the interstitial water molecules) and structure. The initial ammonium metavanadate solutions are prepared in laboratory beakers with a volume of 100 ml by dissolving the needed amount of NH_4VO_3 (from 0.1 to 0.5 g) in 45 ml deionized water at around 30 ºC. Then different volumes of 96% ethanol (0.5, 2.5 and 5 ml, corresponding to 0.42, 2.08 and 4.09 wt.%) are added to the metavanadate solution. Finally, a definite volume of 50 ml of glacial acetic acid is added to each solution. The resulting solution remains clear. Further, at continuous stirring the solution is heated to 50, 70 and 85 ºC accordingly with a heating rate of about 5 ºC/min and the temperature is maintained constant for about 1 h. The precipitates obtained are filtered in hot at the given temperature and dried over night.

Preparation of the Thin Films

The thin films are prepared on commercially available glass substrates of SnO_2:F (FTO) which possess high optical transparency of 80% in the visible spectrum and electrical resistance of 10–20 Ω. Before deposition, the substrates are cleaned in the following sequence: with detergent, alkaline solution, hydrochloric acid, hexane, acetone and finally rinsed with deionized water and dried in air.

Electrochromic thin films of $V_2O_5{\cdot}nH_2O$ xerogels are prepared by a chemical bath deposition method. The solution for the film deposition is obtained following the above described procedure, but without using ethanol. We decided not to use ethanol because of two considerations: (i) the addition of ethanol doesn't influence the xerogel composition as we established (see the next section); (ii) the presence of ethanol, however, could make the film adhesion worse. The thin films under consideration in the present paper are prepared from 0.009 M ammonium metavanadate solution, i.e. using 0.1 g reagent, 45 ml water and 50 ml acetic acid. The deposition is performed in a glass beaker of 100 ml at 75 ºC. The clean substrates are placed vertically supported to the wall of the beaker. The deposition solution is heated to 75 ºC and stirred continuously on a magnetic stirrer. The beginning of the deposition reaction is observed as an appearance of yellow-orange opaque state of the solution which occurs at 70 °C, but the deposition on the substrate is observed when the reaction temperature reaches the value of 75 °C. Operating temperature is maintained up to the end of the chemical deposition, so called deposition time.

The colour of the reaction system at the beginning of the reaction is yellow-orange, but over time becomes orange-brown and at the end of the reaction turns to bright brown. The thin films of $V_2O_5{\cdot}nH_2O$ xerogels are removed from the chemical bath, washed with ethanol and dried at room temperature. The as prepared films are homogeneous, transparent and have yellow colour that varies from light yellow to deep yellow depending on the deposition time. All reagents used are analytical pure substances.

It should be mentioned that the deposition temperature (75 °C) is a little bit higher than the temperature for the precipitate formation (70 °C). But it ensures a higher rate of the deposition without change of the film composition. Thus, by performing the deposition at 75 °C instead of 70 ºC we are able to prepare thin films with different thicknesses for a reasonable deposition time up to 50 min.

Characterization of the solids and thin films

The XRD patterns of the precipitates and thin films were recorded by Rigaku Ultima IV X-ray diffractometer (CuKα radiation). Infrared spectra were obtained with a Perkin-Elmer System 2000 infrared interferometer using KBr disks. The thermal studies of the precipitates (TG and DTA) were carried by LABSYS^{TM} Evo apparatus (SETARAM) in the temperatures up to 500 °C at a heating rate of 10 °C/min in an air flow. The elemental analysis of the precipitates (N and H) was performed using Elementar Analysensysteme GmbH (VarioEL analyser). AFM investigations were made with the instrument NanoScopeV system (Veeco Instruments Inc.) in taping mode at room temperature. The morphology of the thin films was observed by scanning electron microscopy (JEOL JSM-5510). The electrochemical properties were examined by cyclic voltammetry in conventional three-electrode cell using a micro AUTOLAB II equipment (Eco-Chemie, Utrecht, Netherlands) in the potential range between –0.75 and 0.5 V. The prepared thin film is the working electrode, the reference electrode is Ag/AgCl (3 M KCl) and the auxiliary electrode is a platinum wire.

In-situ optical spectra of the thin films are recorded by Varian Cary 50 Scan spectrophotometer in the range from 350 to 900 nm using a 1 M $LiClO_4$ in propylene carbonate (PC) as electrolyte. The voltage is varied from –2.5 to +2.5 V. The FTO spectrum is measured as a background spectrum.

The film thickness was measured by Alpha Step D-100 profilometer (measuring parameters: stylus force 5 mg, length 8 mm, range 10 μm and speed 0.07 mm/s).

Results and Discussion

Precipitation in the System NH_4VO_3-CH_3COOH-C_2H_5OH

The precipitation in the system NH_4VO_3-CH_3COOH-C_2H_5OH was studied in details at three different vanadium and alcohol concentrations and temperatures between 50 and 85 ºC. Table 1 gives information on the precipitation time which is an important experimental factor parameter in respect to the preparation of the

Table 1 Precipitation in the NH_4VO_3-CH_3COOH-C_2H_5OH system.

Exp. No	$V(C_2H_5OH)$ (ml)	T (°C)	$m(NH_4VO_3)$ (g)	$c(NH_4VO_3)$ (mol/dm^3)	Beginning of precipitation (min)	End of precipitation (min)
1	0.5	50	0.1	0.009	*	*
2	2.5	50	0.1	0.009	*	*
3	0.5	70	0.1	0.009	20	45
4	2.5	70	0.1	0.009	17	43
5	0.5	85	0.1	0.009	5	30
6	2.5	85	0.1	0.009	6	30
7	0.5	50	0.3	0.027	12	42
8	2.5	50	0.3	0.027	11	41
9	0.5	70	0.3	0.027	8	32
10	2.5	70	0.3	0.027	7	31
11	0.5	85	0.3	0.027	3	23
12	2.5	85	0.3	0.027	2	22
13	0.5	50	0.5	0.045	1	12
14	2.5	50	0.5	0.045	1	12
15	0.5	70	0.5	0.045	2	17
16	2.5	70	0.5	0.045	2	17
17	0.5	85	0.5	0.045	1	11
18	2.5	85	0.5	0.045	0.5	11

*No precipitation for 60 min

thin films.

Our experiments showed that at low concentration of NH_4VO_3 (0.009 M) at 50 ºC no precipitation occurs up to 60 min, regardless the amount of C_2H_5OH. For this vanadium concentration a reasonable rate of precipitation (in about 20 min) was reached at temperatures higher than 70 ºC. At higher vanadium concentrations, (0.3 and 0.5 g NH_4VO_3 equivalent to 0.027 and 0.045 M), the precipitation already occurs at 50 ºC, the latest in 12 min. In general, the rate of precipitation increases with increase in the vanadium concentration, accordingly temperature and quantity of alcohol, at constant other synthesis parameters. Moreover, it appears that the quantity of alcohol and temperature are more significant at lower vanadium concentration. For example, at vanadium concentration of 0.009 M and 0.5 ml alcohol at 70 ºC the precipitation starts in 20 min, *versus* 5 min at 85 ºC. At five-fold higher vanadium concentration and same quantity of alcohol the precipitation occurs in 1-2 min at all temperatures between 50 and 85 ºC.

Fig. 1 summarizes the XRD patterns of the precipitates obtained in the system NH_4VO_3–CH_3COOH–C_2H_5OH at different concentrations of NH_4VO_3 and 0.5 ml C_2H_5OH between 50 and 85 ºC. In the figure the samples are denoted in the following manner: the first two numbers refer to the amount of NH_4VO_3 (0.1 or 0.3 or 0.5 g), while the last two numbers refer to the temperature of precipitation (50 or 70 or 85 ºC). For example, VA0370 denotes the precipitate obtained from solution containing 0.3 g NH_4VO_3 at 70 ºC.

Analogous XRD patterns were obtained at higher quantity of ethanol (2.5 and 5 ml) as well as without any ethanol (not presented). Therefore, the ethanol does not influence the chemical composition of the precipitates as we initially expected and only the beginning and rate of precipitation are affected by its presence and quantity.

It is seen (Fig. 1) that two types of XRD patterns are observed for all samples. This allows the precipitates obtained to be subdivided into two groups depending on the general view of the XRD pattern. The first group comprises the precipitates obtained from the most dilute vanadium solution (0.009 M) at temperatures between 70 and 85 ºC regardless the amount of ethanol. In their XRD patterns about ten broad peaks are distinguished. The second group includes all other samples obtained from more concentrated vanadium solutions (0.027 and 0.045 M) between 50 and 85 ºC in the presence and not of ethanol in the reaction system. In their XRD patterns very small number of broad and low intense peaks (2 peaks for VA05 and 4-5 peaks for VA03) can be seen. But, if the XRD patterns are recorded at a lower scan rate (1 °/min) then three broad peaks with pronounced first peak are clearly visible as it is demonstrated for VA0550 in Fig. 2. Our further detailed studies showed that the samples from the two groups have different chemical composition. Accordingly, two groups of thin films were prepared under the same experimental conditions as the corresponding precipitates and their optical properties showed a strong dependence on the deposition conditions. Because of that it is more appropriate the two groups of samples to be considered in details separately. The present paper is focused on the

characterization of the thin films and precipitate obtained from the dilute solution of NH_4VO_3 (containing 0.1 g NH_4VO_3) at 75 ºC denoted hereafter as VA0175.

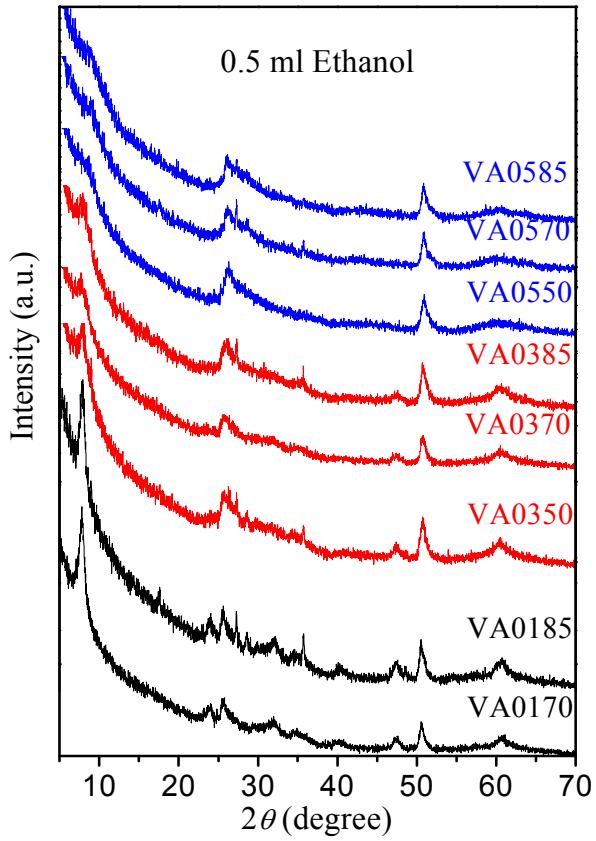

Fig. 1 XRD patterns of the precipitates obtained in the system NH_4VO_3-CH_3COOH-C_2H_5OH at different temperatures and vanadium concentration with 0.5 ml alcohol. The scan rate is 6 º/min. The samples are denoted in the following manner: the first two numbers indicate the amount of NH_4VO_3 (0.1; 0.3; 0.5 g), while the last two numbers indicate the temperature (50; 70; 85 ºC).

Composition and Structure of VA0175

Fig. 2 shows the X-ray powder diffraction patterns of the precipitate VA0175 from the chemical bath and of the film prepared under the same condition without additon of ethanol. Besides the peaks due to FTO substrate the two patterns are practically identical (with exception of a difference in the intensities of some peaks) which evidences the same phase composition of the film and precipitate (Fig. 2). This is of importance since we can undertake some studies that require a bigger amount of the sample (for example TG-DTA analyses, elemental analysis, etc.) using the precipitate, and the obtained data are then referred to the film.

The XRD patterns of VA0175 (Fig. 2) exhibit a small number of broad diffraction peaks, about ten peaks. The first peak centered at 7.88 º (d = 11.22 Å) is much more intense than the other peaks located above 23 º (2θ scale). The comparison with the patterns from PDF database showed that our diffractograms do not correspond exactly to any known X-ray powder patterns of vanadium compounds. However, there is a great similarity with

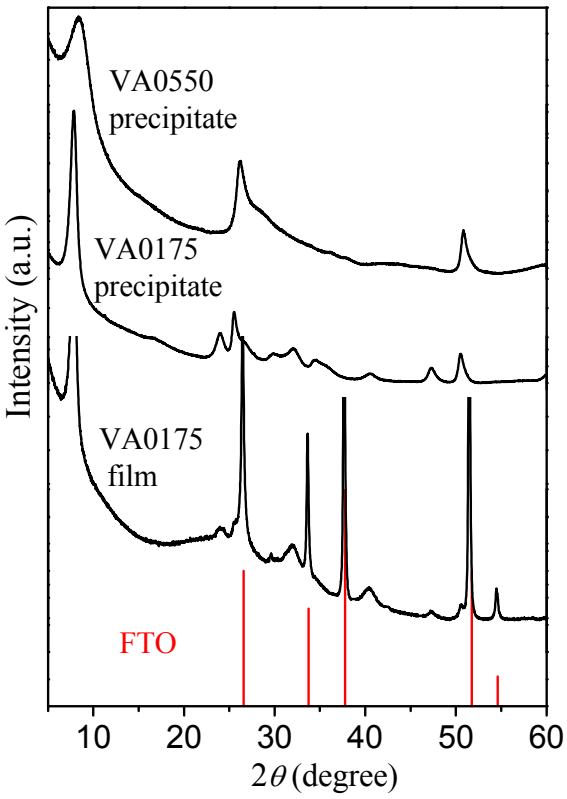

Fig. 2 XRD patterns of VA0175 (film and precipitate) and VA0550 precipitate recorded at scan rate of 1 º/min.

the pattern of pristine $V_2O_5{\cdot}nH_2O$ xerogel (PDF 40-1296) with the difference that our patterns exhibit additional peaks. Moreover, the XRD pattern of VA0175 resembles very much the reported patterns of intercalated xerogels like $(CH_3NH_3)_{0.37}V_2O_5{\cdot}0.33H_2O$[24] and $M_{0.3}V_2O_5{\cdot}1.5H_2O$ (M = Na^+ and TMA^+ (tetramethyl ammonium)).[25]

The structure of xerogel is found to be an assembly of double V_2O_5 sheets forming slabs that are stacked along the *c*-axis of a monoclinic unit cell.[26] The slabs are separated by water molecules. The basal distance between the layers depends on the amount of water and increases by step of about 2.8 Å for each water layer: 11.55 Å for $n \approx$ 1.5-1.6 and 8.75 Å for $n \approx 0.5$.[27] The structural coherence is however limited to about 50 Å (close to the interslab separation) suggesting that the slabs are turbostratically disordered.[26] This determines the typical XRD pattern of the xerogels that is characterized by a small number of 3-5 broad peaks from the series of *00l* reflections (missing *002* peak) with a pronounced *001* peak located generally around 11.5 Å.[5,13,28] It was reported that the intercalation of cations like Na^+ and TMA^+ (tetramethyl ammonium) into the xerogel leads to the appearance of extra diffraction peaks in the diffraction patterns of $M_{0.3}V_2O_5{\cdot}1.5H_2O$.[25] Durupthy et al.[25] have suggested that the observation of *hkl* set of reflections (instead of *00l* only) is related to the loss of ordered stacking of the double V_2O_5 layers. Similar considerations can be supposed for our synthesis material since its diffractogram resembles to great extent the patterns of $M_{0.3}V_2O_5{\cdot}1.5H_2O$.[25] Because of all above we consider that the NH_4^+ ions present in the reaction system are accommodated into the V_2O_5 xerogel framework during the precipitation process resulting in the formation of NH_4^+ intercalated vanadium(V)

oxide xerogel, $(NH_4)_xV_2O_5{\cdot}nH_2O$. This is in line with the fact that the layered structure $V_2O_5.nH_2O$ xerogel serves as a versatile host matrix for the intercalation of a large variety of guest ionic and molecular species.[5,25,29-32] The incorporation of cations between the layers is as a result of ion-exchange reactions with the acid protons of the gels, so the amount of the intercalated ions is usually around 0.3-0.4 per mole of V_2O_5.[25,29,30,33] However, for our $(NH_4)_xV_2O_5{\cdot}nH_2O$ precipitate the elemental analysis gives a lower content of ammonium ions, x = 0.12-0.15, probably related with the low concentration of the initial reagent NH_4VO_3 in the reaction system (0.009 M).

The formation of xerogel in both forms, film and precipitate, is further supported by the IR spectra of the precipitate and scraped

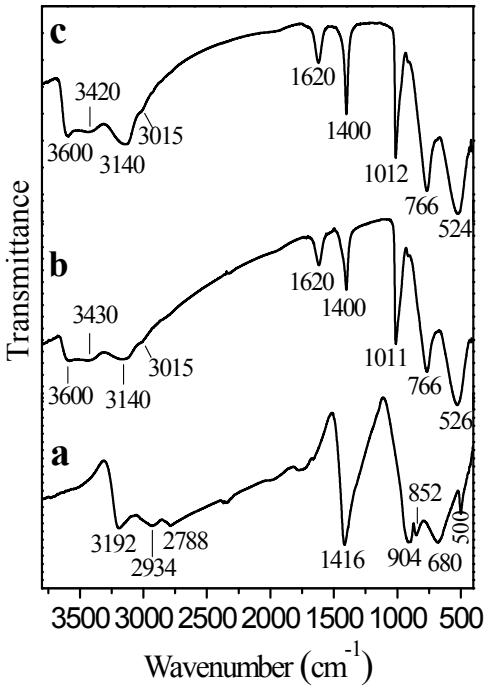

Fig. 3 IR spectra of (a) NH_4VO_3, (b) VA0175 precipitate and (c) VA0175 film.

film (Fig. 3b and c) which are the same (within the limits of the experimental resolution), thus confirming their same composition. In addition, both IR spectra are different from that of the initial reagent NH_4VO_3 (Fig. 3a).

The IR spectra of the as-deposited gels display the three characteristic vibrational bands of the V_2O_5 framework of the xerogels[32,34,35] around 1000, 760 and 500 cm^{-1} as well as the bands due to the water molecules residing in the interlayer space.[34,36] The band at 1011 cm^{-1} is attributed to the stretching vibration of terminal V=O groups (shorter V–O bond), the band at 766 cm^{-1} is due to asymmetric stretching vibration of the bridged V–O–V units (longer V–O bonds), and the band at 526 cm^{-1} is assigned to the V-O-V symmetric stretch mixed with bending vanadium oxygen vibrations.[32,34,36] The band near 3600 cm^{-1} is supposed to be due to the OH stretching vibrations of two types of water molecules. The one type comprises water molecules nearly free of hydrogen bonding which are presumably directly bonded to vanadium through their oxygen atom,[34,36] while the other type represents the water molecules trapped into the cavities of the lattice.[34,35] The band at 3430 cm^{-1} is attributed to the water molecules hydrogen bonded with the oxygen of V_2O_5[34,37] or of other H_2O molecules[34,36] and the band at 1620 cm^{-1} is the H-O-H bending vibration.

Besides the commented vibrational bands our IR spectra clearly show additional bands due to the vibrations of NH_4^+ ions[38]: N-H stretching vibrations at 3140 and 3015 cm^{-1} (shoulder) and H-N-H bending vibration at 1400 cm^{-1}. This observation unequivocally confirms the presence of the NH_4^+ ions in the xerogel framework. It is worth mentioning that the positions of the three main bands associated with the V-O units are very close to these for pristine $V_2O_5{\cdot}nH_2O$ xerogels: 1015, 760 and 515 cm^{-1}.[34–36,39] This finding shows that the V_2O_5 framework in $(NH_4)_{0.15}V_2O_5{\cdot}nH_2O$ is not perturbed by the intercalated ammonium ions, probably due to their comparatively low content. This is not true, however, when the content of NH_4^+ is increased as revealed by our studies of the gels prepared under other synthesis conditions (forthcoming paper).

The thermal behaviour of $(NH_4)_{0.15}V_2O_5{\cdot}nH_2O$ was studied by TG-DTA technique. Before the discussion for a greater precision it is necessary to note that the experimental mass loss will consider both water (main component) and ammonium ions (minor component) since the product of thermal heating of the gel is V_2O_5 (see further). However, we are not able to separate the

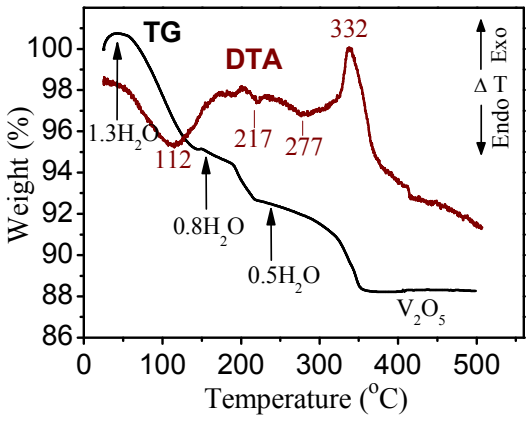

Fig. 4 TG-DTA curves for VA0175 precipitate.

water and ammonium ions. Moreover, the amount of the ammonium ions is low (0.15 moles) and for simplicity they will be ignored in the next considerations. But, their amount is finally taken into account when calculating the water amount.

According to TG and DTA curves (Fig. 4) the dehydration of the xerogel occurs in three separate steps in accord with earlier reports.[27,34] The first step is developed in the temperature range of 40–150 ºC (endothermic peak at 112 ºC) with a mass loss of 5.71 wt.% formally equivalent to 0.65 mole H_2O. These water molecules are the most weakly bonded ones. The second step is observed between 150 and 230 ºC with endothermic peak at 217 ºC and it is characterized by a mass loss of 2.66 % corresponding to 0.30 mole H_2O. The last amount of strongly retained water molecules, 4.14 wt.% equivalent to 0.50 mole H_2O, is released between 250 and 360 ºC (third step) and the endothermic effect at 277 ºC is related to this process. The last endothermic effect is immediately followed by an exothermic peak at 332 ºC due to the crystallization of orthorhombic V_2O_5 (PDF 41-1426). The TG

curve gives a total mass loss of 12.50 wt.% that formally corresponds to 1.44 mole of water. Subtracting the amount of the released ammonium ions (0.15 moles) we obtain a precise amount of the water content of 1.3 moles i.e. the composition of as prepared xerogel is $(NH_4)_{0.15}V_2O_5{\cdot}1.3H_2O$ and, accordingly the intermediate xerogels are $(NH_4)_{0.15}V_2O_5{\cdot}0.8H_2O$ (at 150 ºC) and $(NH_4)_{0.15}V_2O_5{\cdot}0.5H_2O$ (at 230 ºC). This means that the water amount is a little bit smaller than the usual, around 1.5 moles, but it is in agreement with the observed d-spacing of 11.20 Å, the latter being also smaller than the usual 11.55 Å.

From XRD, IR spectroscopy and TG–DTA data we can conclude that the synthesis product labeled as VA0175 under the form of film and precipitate is a vanadium oxide xerogel with a composition $(NH_4)_{0.15}V_2O_5{\cdot}1.3H_2O$.

Thickness and Morphology of $(NH_4)_{0.15}V_2O_5{\cdot}1.3H_2O$ Thin Films

By varying the deposition time from 10 min to 50 min a series of thin films of $(NH4)_{0.15}V_2O_5{\cdot}1.3H_2O$ with different thickness were prepared. As expected the film thickness increases with the increased deposition time (Fig. 5). The thinnest film with 150 nm thickness was obtained for 10 min of deposition time, while the thickest film of about 320 nm was obtained for 50 min deposition time. Films with thicknesses of about 150, 210, 280 and 320 nm were used for electrochemical and optical studies.

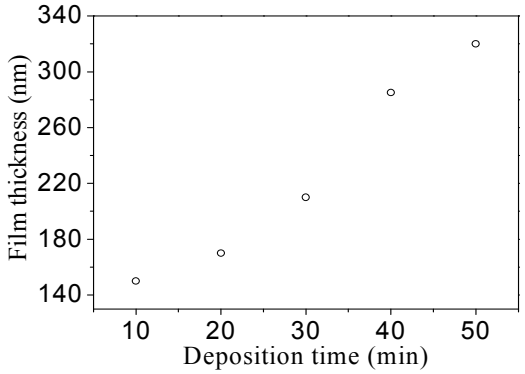

Fig. 5 Film thickness *vs* deposition time.

Fig. 6 display two SEM images with different magnification of the surface of the $(NH_4)_{0.15}V_2O_5{\cdot}1.3H_2O$ thin film with a thickness of 210 nm. It is seen that the surface of the substrate is well populated with the deposited material. At a higher magnification (Fig. 6b) randomly oriented ribbon-like particles which are about 150 nm wide and 500 nm long are visible. The observation of ribbon-like structure of the prepared vanadium oxide xerogels is in accordance with previous results.[25,2]

Part of the 2D surface topography of the same $(NH_4)_{0.15}V_2O_5{\cdot}1.3H_2O$ thin film (210 nm thickness) is shown in Fig. 7. The film surface is well populated by grains having sizes between 50 and 100 nm. The grains are tightly stuck to each other forming elongated aggregates with length between 100 and 300 nm. Based on this observation we can conclude that the ribbons

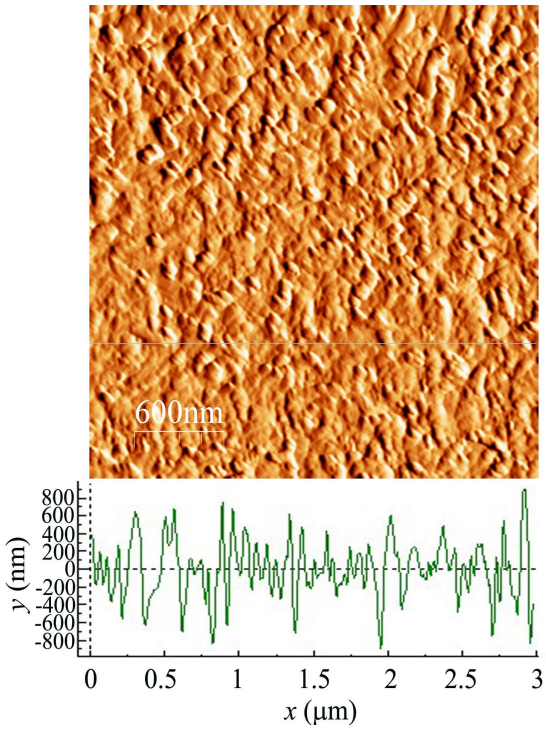

Fig. 7 AFM image and profile of the $(NH_4)_{0.15}V_2O_5{\cdot}1.3H_2O$ thin film with 210 nm thickness.

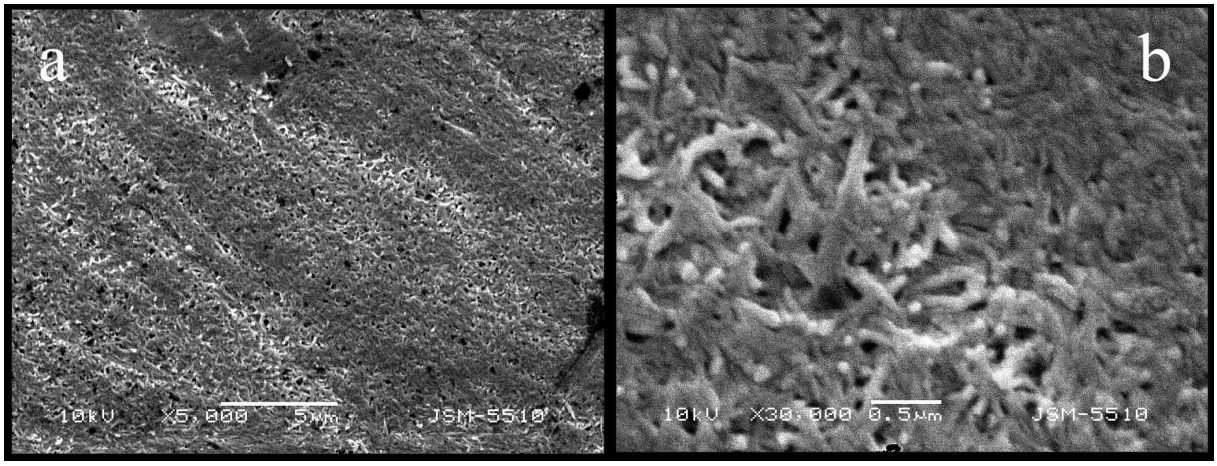

Fig. 6 Scanning electron micrographs of the $(NH_4)_{0.15}V_2O_5{\cdot}1.3H_2O$ thin film with 210 nm thickness.

observed by SEM are actually composed by aggregated primary nanoparticles. The film exhibits a high roughness and the amplitude of grains height is around 900 nm (Fig. 7).

Electrochemical properties

The electrochemical properties of the prepared thin films are studied by cyclic voltammetry in the potential range between –1 and +1 V (vs. Ag/Ag+) at a scanning rate of 10 mV/s in 1 M $LiClO_4$/PC as electrolyte. The measured area of the films is 0.32 cm^2.

Five voltammograms of two $(NH_4)_{0.15}V_2O_5{\cdot}1.3H_2O$ thin films with different thickness are shown in Fig. 8. Two peaks for both reduction and oxidation processes are observed for the thinner film (Fig. 8a) which is in agreement with previous studies on vanadium(V) oxide xerogels.[40,41] With an exception of the first scan (Fig. 8a), the remaining four scans have cathodic peaks at –0.13 and –0.45 V, and anodic peaks at –0.19 and 0.08 V. In the case of the thicker films having thickness larger than 150 nm (Fig. 8b), the cyclic voltammograms exhibit also two cathodic peaks with slightly different potentials (–0.15 and –0.50 V), but only one anodic peak at –0.05 V. The latter peak is very broad and has an intermediate position between the two anodic peaks observed at the cyclic voltammograms of the thinner film. Because of that we supposed that this peak is a result of overlapping of two unresolved anodic peaks (analogous to these for the thinner film) related to some kinetic hindrances due to

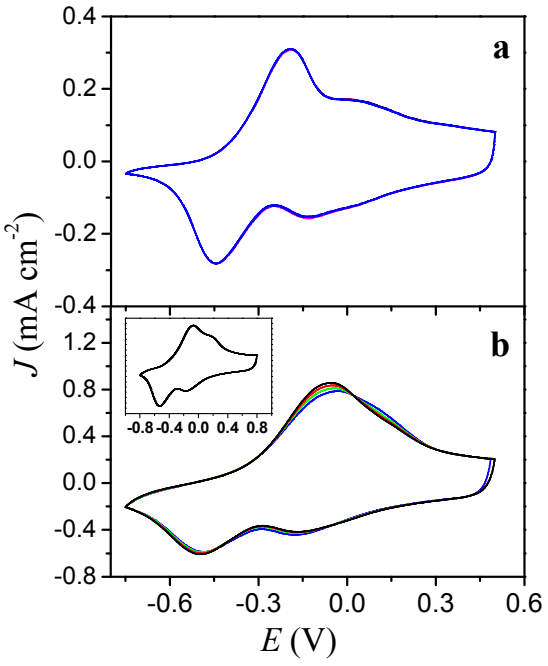

Fig. 8 Five cyclic voltammograms of thin films of $(NH_4)_{0.15}V_2O_5{\cdot}1.3H_2O$ with thickness of (a) 150 nm and (b) 210 nm recorded at 10 mV/s. The inset shows data recorded at 5 mV/s.

larger thickness. Indeed, at a lower scan rate of 5 mV/s two anodic peaks become visible during the anodic sweep (inset in Fig. 8b).

The cyclic voltammetry experiments show that the lithium ions are reversibly intercalated in two steps during the cathodic potential sweep and deintercalated by the subsequent anodic sweep. Accordingly, reversible reduction/oxidation processes between V(V) and V(IV) sites take place which give rise to reversible colour transformations.

For both films the peak observed at higher potential for given process (reduction or oxidation) corresponds to the faster reaction (narrower peak), while the peak at lower potential for given process represents the slower reaction (broader peak). As a whole the reduction process is slower than the oxidation one.

In the literature different number pairs (one, two and three) of oxidation/reduction peaks are reported to appear in the cyclic voltammograms of vanadium oxide thin films.[2,40,42] The observation of one redox pair has been attributed to the amorphous nature of the films.[42] Most often two redox pairs are found in the CV curves of vanadium(V) oxide xerogels[40,41] and according to Benmoussa et al.[40] the appearance of two redox pairs reflects the crystalline nature of the films. Most recently, Costa et al.[2] have observed three redox pairs. The physical explanation of the two and three redox pairs is related to the step-wise reduction/oxidation processes between V(V) and V(IV) sites and formation of different crystalline states $Li_xV_2O_5$.[2,40,41,43] As reported in the concentration limits $0 < x < 1$ lithium is reversibly

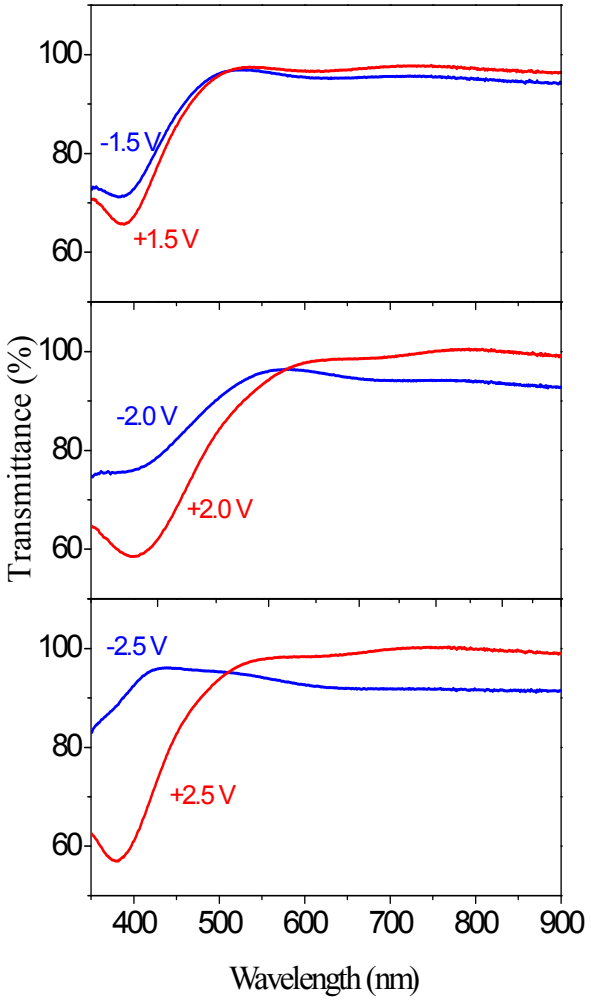

Fig. 9 Optical transmittance spectra of thin film of $(NH_4)_{0.15}V_2O_5{\cdot}1.3H_2O$ with 150 nm thickness at different voltages.

inserted/extracted giving rise to three distinct states (α, ε, δ phases), while at higher lithium content $1 < x \leq 2$ some structural reorganizations take place corresponding to partially irreversible phases.[2,41,43]

Optical properties

Fig. 9 shows the optical transmittance spectra of thin film with 150 nm thickness at different applied voltages: –1.5/+1.5 V; –2.0/+2.0 V; –2.5/+2.5 V. As seen the increased voltage results in the increased values of the transmittance variation (ΔT) achieved for the same time of 1 min. The transmittance variance is defined as a difference in the transmittance of the two redox states of the film at given wavelength. So, the further studies of the optical properties are performed at applied voltages of –2.5 (reduction) and +2.5 V (oxidation).

In order to determine the optimal time for the reduction and oxidation a kinetic study is performed at $\lambda = 400$ nm. The voltage polarity was switched every one minute for the film with thickness 150 nm and every 2 min for the film with thickness 210 nm. The absorbance is measured as an optical response on the redox processes and the results are shown in Fig. 10. As expected the changes are slower in the case of the thicker film. For both films the oxidation is significantly faster process than the reduction one which confirms our conclusions derived from the electrochemical experiments.

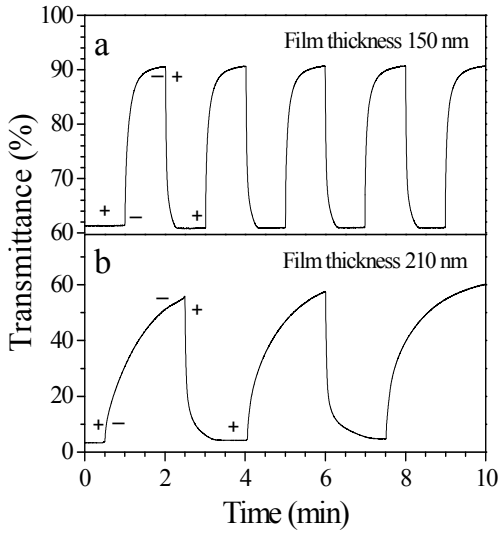

Fig. 10 Optical transmittance at 400 nm *vs* time at applied voltages of –2.5 and +2.5 V for the thin films with different thicknesses of (a) 150 nm and (b) 210 nm.

For instance, in case of the thinner film the oxidation is almost three times faster than the reduction. From these results it follows that the optimal time for measurements of the transmittance spectra of thin films with thickness of 150 nm is 1 min, while a longer time is needed for the thicker films.

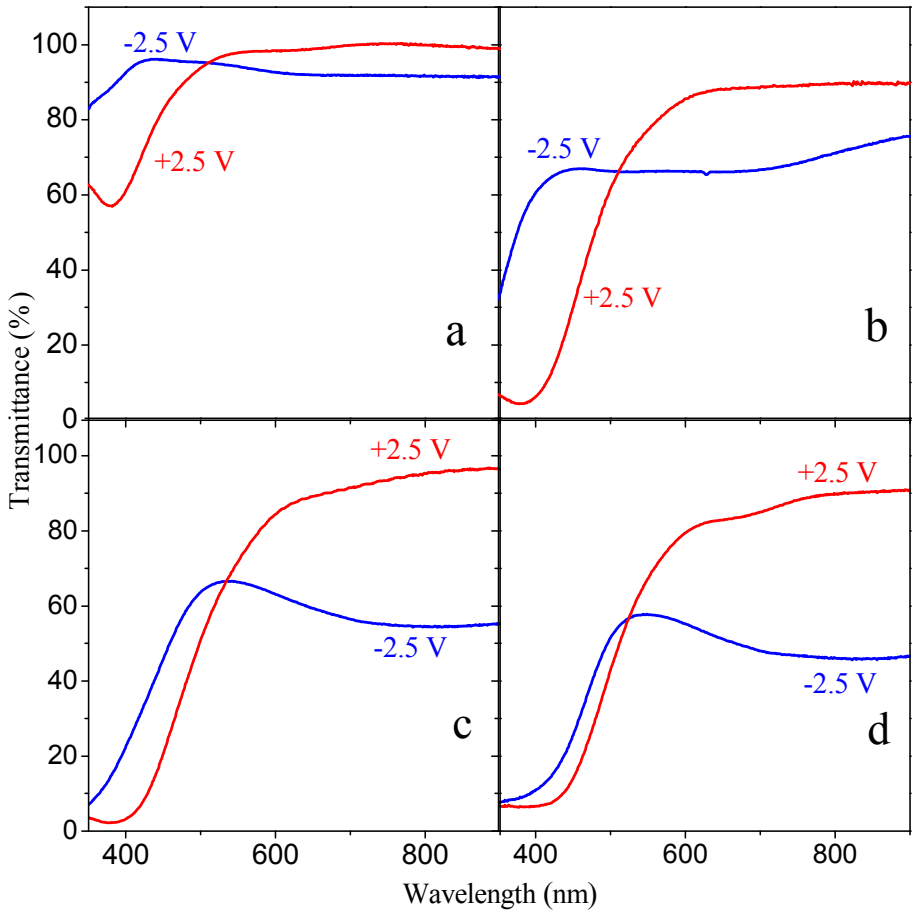

Fig. 11 *In-situ* optical transmittance spectra of thin films of $(NH_4)_{0.15}V_2O_5 \cdot 1.3H_2O$ with different thicknesses of (a) 150 nm, (b) 210 nm, (c) 280 nm and (d) 320 nm.

The optical transmittance spectra of a series of the thin films with different thickness at potentials of –2.5 V and +2.5 V applied for 2 min are shown in Fig. 11. The four films exhibit two-step electrochromism with noticeable colour transformations, yellow/green and green/blue which is comparable with the observation of two redox pairs in the cyclic voltammograms.

The transmittance variance deduced from each pair of optical spectra of the films with different thickness at three wavelengths (400, 750 and 900 nm) is given in Table 2. The ΔT values in Table 2 are average values taken from ten measurements of a film with given thickness.

The results obtained indicate that the transmittance variance at a given wavelength strongly depends on the film thickness, but the relationship between ΔT and the film thickness does not follow an universal trend. At 400 nm ΔT variation passes through a maximum of 54% for the film with 210 nm thickness that is our best achievement among the thin films examined. At 750 and 900 nm ΔT gradually increases with the increased film thickness and the films with 280 and 320 nm thickness exhibit also very good ΔT values around 41-44%. In the last cases, however, we established that the thick films can be readily removed by wiping with cotton after the optical measurements. Since, all studied films before the electrochemical measurements have passed an adhesion tape test, we suppose that the worse adhesion is result of the electrochemical transformation during the cycling in the electrolyte.

Regarding the transmittance variance in electrochromic vanadium oxides we have found the following published data: 20% (at –0.4 and 1.6 V),[44] 25% (at –0.4 and 1.2 V),[40] 25% (at –1.5 and 2 V),[45] 27% (at 1.8 and 3.6 V),[46] 40% (at –1.5 and 1.5 V),[2] and 40% (at –0.6 and 0.9 V)[47] The best performance is reported by Scherer et al.[48] for a mesoporous film of vanadium oxide with ΔT around 50% (at –1 and +1 V), very high colouration efficiency of 3500 cm^2/C, stability up to 10^2 cycles with 20% degradation. Evidently, our data are obtained at higher potentials compared to those used in the literature. In spite of that our best achievement for ΔT around 54% is highly valuable. It is likely that the good result for ΔT can be related, at least partially, to the film morphology that comprises ribbon-like units composed of nanoparticles with dimensions between 50 and 100 nm.

Conclusions

The precipitation in the NH_4VO_3–CH_3COOH–C_2H_5OH system has been studied at three vanadium and ethanol concentrations and temperatures between 50, 70 and 85 ºC. Depending on the metavanadate concentration and temperature two groups of ammonium intercalated vanadium(V) oxide xerogels with different chemical composition are obtained. It is established that the ethanol does not influence the composition of the xerogels, but it affects the beginning and rate of the precipitation.

Thin films on FTO substrates with composition $(NH_4)_{0.15}V_2O_5{\cdot}1.3H_2O$ have been prepared by a newly developed chemical bath deposition method based on the acidification of a dilute aqueous solution of NH_4VO_3 and acetic acid at 75 ºC. This method is very simple and cheap (it does not require sophisticated instruments), the preparation parameters are easily controlled and the low-temperature deposition allows the use of polymer substrates. In addition, it can be easily adopted for a large and small area deposition.

The composition and structure of both solids and thin films are examined by X-ray diffraction, IR spectroscopy and TG-DTA analyses. As evidenced by SEM and AFM studies the film morphology is characterized by randomly oriented ribbon-like units composed of aggregated nano-particles with dimensions in the region of 50–100 nm. The electrochemical properties and electrochromic activity of a series of thin films with thickness between 150 and 320 nm have been studied in 1 M $LiClO_4$ in propylene carbonate (PC) as electrolyte. The cyclic voltammograms display two relatively stable redox pairs which correspond to the two-step electrochromism with colour transformations yellow/green and green/blue. It is established that the film thickness strongly influences the transmittance variance at given wavelength as deduced by the optical spectra of the reduced and oxidized states of the films. The films having a thickness of about 300 nm show good values of the transmittance variance of 41–44% at 750 and 900 nm. Among the studied thin films the highest value of the transmittance variance of 54% at 400 nm is achieved for the film with thickness about 200 nm. The obtained data for the electrochromic activity of ammonium intercalated vanadium(V) xerogel thin films prepared by chemical bath deposition method are promising for their potential application in electrochromic devices.

Acknowledgment

The authors are grateful to Alexander von Humboldt Stiftung for providing the electrochemical equipment without which the present study would not have been possible.

Notes

[a] *Institute of Chemistry, Faculty of Natural Sciences and Mathematics, Ss. Cyril and Methodius University, POB 162, Arhimedova 3, 1000 Skopje, Republic of Macedonia, Fax: 389 2 3226865; Tel: +389 78 570700; E-mail: metonajd@pmf.ukim.mk*

[b] *Institute of General and Inorganic Chemistry, Bulgarian Academy of Sciences, Acad. G. Bonchev Str. Bldg. 11, 1113 Sofia, Bulgaria. E-mail: vkoleva@svr.igic.bas.bg*

See DOI: 10.1039/b000000x/

References

1 D. S. Shang, L. Shi, J. R. Sun and B. G. Shen, *J. Appl. Phys.,* 2012, **111**, 053504.
2 C. Costa, C. Pinheiro, I. Henriques and C. A. T. Laia, *Appl. Mater. Interfaces*, 2012, **4**, 5266−5275.
3 C. M. Amb, A. L. Dyer and J. R. Reynolds, *Chem. Mater*., 2011, **23**, 397−415.
4 J. D. Lee, *Concise Inorganic Chemistry*, Chapman & Hall, England, 1996.
5 J. Livage, *Chem. Mater*., 1991, **3**(4), 578-593.
6 N. V. Vivier, S. Belair, C. C. Vivier, J. Y. Nedelec and L. T. Yu, *J. Power Sources*, 2001, **103**, 61–66.
7 E. A. Olivetti, J. H. Kim, D. R. Sadoway, A. Asatekin and A. M. Mayes, *Chem. Mater.*, 2006, **18**, 2828-2833.
8 K. Jeyalakshmi, S. Vijayakumar, S. Nagamuthu and G. Muralidharan, *Mater. Res. Bull.*, 2013, **48**, 760–766.
9 M. Macalík, J. Vondrák, M. Sedlaříková, J. Mohelníková and R. Helan, *6th Advanced Batteries and Accumulators – ABA*, 2005.
10 R. Ceccato and G. Carturan, *J. Sol-Gel Sci.Technol.*, 2003, **26**, 1071–1074.

11 J. Scarminio, A. Tallledo, A. Andersson, S. Passerini and F. Deckers, *Electrochim. Acta.*, 1993, **38**(12), 1637-1642.
12 S. T. Lutta, H. Dong, P. Y. Zavalij and M. S. Whittingham, *Mater. Res. Bull.*, 2005, **40**, 383–393.
13 R. Ceccato, S. Dirè, T. Barone, G. De Santo and E. Cazzanelli, *J. Mater. Res.,* 2009, **24**(2), 475- 481.
14 J. Livage, F. Beteille, C. Roux, M. Chatry and P. Davidson, *Acta mater*., 1998, **46**(3), 743-750.
15 B. Alonso and J. Livage, *J. Solid State Chem.*, 1999, **148**, 16-19.
16 Z. Li, Y. Zhang and Z. Shi, *Int. J. Mater. Res.*, 2013, **06**, 567-572.
17 Y. Hana, I. Choia, H. Kangb, J. Parkb, K. Kimb, H. Shinb and S. Moonb, *Thin Solid Films*, 2003, **425**, 260–264.
18 L. Ottaviano, A. Pennisi, F. Simone and A.M. Salvi, *Opt. Mater.*, 2004, **27**, 307–313.
19 K. Takahashi, S. J. Limmer, Y. Wang and G. Cao, *J. Phys. Chem. B*, 2004, **108**, 9795-9800.
20 G. J. Fang, Z. L. Liu, Y. Q. Wang, H. H. Liu and K. L. Yao, *J. Phys. D: Appl. Phys.*, 2000, **33**, 3018–3021.
21 M. Najdoski, V. Koleva and S. Demiri, *Mater. Res. Bull*., 2011, **47**(3), 737–743.
22 M. Najdoski, V. Koleva, S. Demiri and S. Stojkovikj, *Mater. Res. Bull.*, 2012, **47**, 2239-2244.
23 S. Stojkovikj, M. Najdoski, V. Koleva and S. Demiri, *J. Phys. Chem. Solids.*, 2013, **74**, 1433–1438.
24 R. J. Chen, P. Y. Zavalij, M.S. Whittingham, J. E. Greedan, N. P. Raju and M. J. Bieringer, *Mater. Chem.,* 1999, **9**, 93-100.
25 O. Durupthy, N. Steunou, T. Coradin, J. Maquet, C. Bonhomme and J. Livage, *J. Mater. Chem.*, 2005, **15**, 1090-1098.
26 V. Petkov, P. N. Trikalitis, E. S. Bazin, S. J. L. Billinge, T. Vogt and M. G. Kanatzidis, *J. Am. Chem. Soc.*, 2002, **124**, 10157-10162.
27 P. Aldebert, N. Baffier, N. Gharbi and J. Livage, *Mat. Res. Bull*., 1981, **16**, 669-676.
28 J. Livage, F. Beteille, C. Roux, M. Chatry and P. Davidson, *Acta Mater.*, 1998, **46**, 743-750.
29 L. Znaidi, N. Baffier and D. Lemordant, *Solid State Ionics*, 1988, **28–30**, 1750–1755.
30 Y. J. Liu, J. A. Cowen, T. A. Kaplan, D. C. Degroot, J. Schindler, C. R. Kannewurf and M. G. Kanatzidis, *Chem. Mater.*,1995, **7**, 1616-1624.
31 Y. J Liu, J.L.Schindler, D.C. DeGroot, C.R. Kannewurt, W. Hirpo and M.G. Kanadzidis, *Chem. Mater*., 1996, **8**, 524-534.
32 M. Malta, G. Louarn, N. Errien and R. M. Torresi, *J. Power Sources*, 2006, **156**, 533-540.
33 V. L. Volkov and G. S. Zakharova, *Russ. J. Inorg. Chem*., 2009, **54**, 38-41.
34 L. Abello, E. Husson, Y. Repelin and G. Lucazeau, *J. Solid State Chem*., 1985, **56**, 379-389.
35 Y. Repelin, E. Husson, L. Abello and G. Lucazeau, *Spectrochim. Acta*, 1985, **41**A, 993-1003.
36 C. Sanchez, J. Livage and G. Lucazeau, *J. Raman. Spectrosc*., 1982, **12**, 68-72.
37 M. T. Vandenborre, R. Prost, E. Huard and L. Livage, *Mat. Res. Bull.,* 1983, **18**, 1133-1142.
38 K. Nakamoto*, Infrared and Raman Spectra of Inorganic and Coordination Compounds*, John Wiley and Sons, New York, 1986.
39 A. Jin, W. Chen, Q. Zhu, Y. Yang, V. L. Volkov and G. S. Zakharova, *Solid State Ionics,* 2008, **179**, 1256-1262.
40 M. Benmoussa, A. Outzourhit, R. Jourdani, A. Bennouna and E. L. Ameziane, *Active and Passive Elec. Comp.*, 2003, **26**, 245–256.
41 N. T. Bay, P.M. Tien, S. Badilescu, Y. Djaoued, G. Bader, F.E. Girouard,V. V. Truong and L. Q. Nguyen, *J. Appl. Phys.,* 1996, **80**, 7041−7045.
42 J. Livage, *J. Coord. Chem. Rev.*, 1999, **190–192**, 391–403.
43 S. F. Cogan, N. M. Nguyen, S. J Perrotti and R. D. Rauh, *J. Appl. Phys*., 1989, **66**, 1333-1337.
44 N. Ozer, S. Sabuncu and J. Cronin, *Thin Solid Films*, 1999, **338**, 201−206.
45 O. Z. Crnjak and I. Musevic, *Nanostruct. Mater.*, 1999, **12**, 399−404.
46 N. Ozer, *Thin Solid Films*, 1997, **305**, 80−87.
47 W. Zhongchun, C. Jiefeng and H. Xingfang, *Thin Solid Films,* 2000, **375**, 238−241.
48 M. R. J Scherer, P. M. S. Cunha, O. A. Scherman and U. Steiner, *Adv. Mater.,* 2012, **24**, 1217−1221.